efficient of $\partial^2 E/\partial u^2$ in (43) vanishes, *i.e.*,

$$k_1^2 - \mu_0\epsilon_0\omega_1^2 - \mu_0\epsilon_1\omega_1^2 \cos u_0 = k_1^2\left(1 - \frac{v_1^2}{v_L^2(u_0)}\right) = 0. \quad (47)$$

The existence of real u_0 in this range is seen by rewriting (47) as

$$\cos u_0 = \frac{\epsilon_0}{\epsilon_1}\left[\frac{k_1^2/\omega_1^2}{\mu_0\epsilon_0} - 1\right]; \quad (48)$$

hence, u_0 is real if

$$\frac{\epsilon_0}{\epsilon_1}\left|\frac{(k_1/\omega_1)^2}{\mu_0\epsilon_0} - 1\right| \leq 1, \quad (49)$$

or

$$\frac{\epsilon_0}{\epsilon_1}\,|D_\infty| \leq 1,$$

which is identical with (46).

The vanishing of the coefficient of $\partial^2 E/\partial u^2$, however, gives rise to a singularity of the differential equation (45). The singularity arises because even though the values of E and $\partial E/\partial u$ are given on the line $u = u_0$ for all t', the values of $\partial^2 E/\partial u^2$ are not determined by the differential equation (45), and $\partial^2 E/\partial u^2$ may jump across the line $u = u_0$. Hence, the "sonic lines," for which $v_1^2 = v_L^2(u_0)$, are singular lines of the differential equation (45). On each side of such a sonic line a different solution will exist, neither of which can be analytically continued across the sonic line. The sufficiency condition (17), therefore, eliminates the occurrence of such a singularity and guarantees the existence of square-integrable solutions of (45).

ACKNOWLEDGMENT

The authors wish to thank Prof. H. Kurss of the Polytechnic Institute of Brooklyn for helpful discussions regarding the question of convergence.

A New Broad-Band Absorption Modulator for Rapid Switching of Microwave Power*

FRANK REGGIA†, SENIOR MEMBER, IRE

Summary—This paper describes a new technique for obtaining a broad-band absorption modulator for high-speed switching or amplitude modulation of microwave power. This ferrite modulator, an outgrowth of the longitudinal-field rectangular-waveguide phase shifter,[1] has electrical characteristics particularly desirable in a microwave switch. These include a zero-field insertion loss of approximately 0.5 db in the ON state, an isolation of greater than 60 db in the OFF state which is nearly independent of the magnetic control field in this state, and a nearly matched input impedance for all values of applied field. These electrical characteristics are nearly constant over a 30 per cent bandwidth at *X* band. Also, it is possible to design the amplitude modulator to have negligible phase shift at the desired operating frequency.

Other characteristics of this ferrite modulator include small physical size, magnetic control fields of less than 50 oersteds, operating temperatures up to 150°C, and a capability of less than one μsec switching time.

* Received by the PGMTT, March 9, 1961; revised manuscript received, May 3, 1961.

† Diamond Ordnance Fuze Labs., Washington, D. C.

[1] F. Reggia and E. G. Spencer, "A new technique in ferrite phase-shifting for beam scanning of microwave antennas," PROC. IRE, vol. 45, pp. 1510–1517; November, 1957.

INTRODUCTION

IN its most general form, the relationship between the induced RF flux density $\boldsymbol{b}$ and the internal RF magnetic field $\boldsymbol{h}$ in an arbitrarily magnetized polycrystalline-ferrite medium is a permeability tensor given by

$$\begin{bmatrix} b_x \\ b_y \\ b_z \end{bmatrix} = \begin{bmatrix} \mu_{xx} & \mu_{xy} & \mu_{xz} \\ \mu_{yx} & \mu_{yy} & \mu_{yz} \\ \mu_{zx} & \mu_{zy} & \mu_{zz} \end{bmatrix} \begin{bmatrix} h_x \\ h_y \\ h_z \end{bmatrix}. \quad (1)$$

From this expression, Rado[2] has shown that for an unsaturated ferrite medium at microwave frequencies and a dc magnetic field applied in the z direction, the permeability tensor reduces to

$$[\mu] = \begin{bmatrix} \mu & -jK & 0 \\ +jK & \mu & 0 \\ 0 & 0 & \mu_z \end{bmatrix}, \quad (2)$$

[2] G. T. Rado, "Electromagnetic characterization of ferromagnetic media," IRE TRANS. ON ANTENNAS AND PROPAGATION, vol. AP-4, pp. 512–525; July, 1956.

where μ, K, and μ_z are the components in the three mutually perpendicular directions and are complex quantities. Thus,

$$b_x = \mu h_x - jKh_y$$
$$b_y = jKh_x + \mu h_y$$
$$b_z = \mu_z h_z. \tag{3}$$

As seen from the first two equations of (3), an RF magnetic field h_x in the x-direction induces a component of the RF flux density b_x which is proportional to μ and, due to the electron spins precessing about the direction of the dc magnetizaton, also induces a component b_y in the y-direction proportional to K. The operation of the absorption modulator which will be described later depends primarily upon the variation of this latter permeability component K with applied magnetic field.

By making certain approximations, valid only for a low-loss ferrite medium at microwave frequencies and for applied magnetic fields below magnetic saturation, the real part of K is given in terms of the magnetic properties of the medium by

$$K' = -\frac{4\pi M\gamma}{\omega}, \tag{4}$$

where M is the dc magnetization in the direction of the applied magnetic field, $\gamma = 2.8$ Mc/sec-oersteds is the gyromagnetic ratio of the electron for a ferrite medium and ω is the operating angular frequency.

This expression agrees very well with experimental results,[3] shown in Fig. 1, which were obtained at 9340 Mc for a low-loss MgMn ferrite[4] vs the internal dc magnetic field below magnetic saturation. Only the real parts are shown, the imaginary parts are small in comparison. These results were obtained by microwave-cavity perturbation techniques, and the measurements of M vs the applied magnetic field H were obtained by standard ballistic galvanometer techniques.

As seen in Fig. 1, the coupling coefficient K' is zero when no external magnetic field is applied. Since $\mu' = \mu_z' = 0.76$ for this case, the ferrite medium exhibits a scalar permeability with no dispersion to the microwave energy. This intitial permeability of less than unity at X-band is due to the gyromagnetic resonance of electron spins in the internal crystalline anisotropy field of the ferrite.

When the dc biasing field is applied to this ferrimagnetic medium, K' increases to approximately 0.67 at magnetic saturation, at which time the other two components approach unity. It is this variation of K' with applied magnetic field which accounts for the transfer of the incident microwave energy of one polarization to another perpendicular wave in a magnetized ferrite medium. If this perpendicular RF field, which is generated inside a magnetized ferrite, could be attenuated without appreciable loss to the microwave energy which exists in the medium when unmagnetized, it would be possible to design an amplitude modulator with an attenuation characteristic similar to the curve shown for K'. This was done[5] by placing a very thin resistive film inside a relatively large ferrite rod used in the rectangular-waveguide absorption modulator which follows.

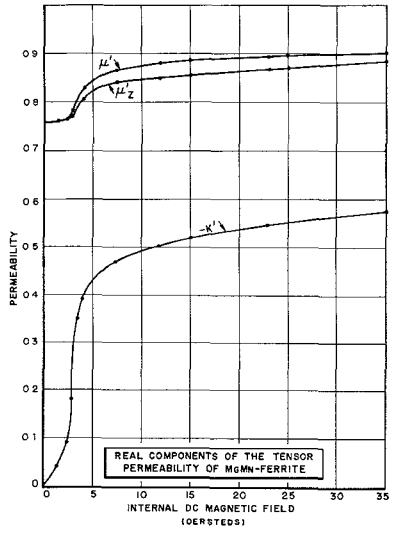

Fig. 1—The three components of the tensor permeability at 9340 Mc vs applied magnetic field below magnetic saturation for a low-loss MgMn ferrite.[4]

Broad-Band Absorption Modulator

A cross-sectional view of the absorption modulator (or microwave switch) making use of the gyromagnetic phenomena described above is shown at the left of Fig. 2. It consists of a low-loss MgMn ferrite rod (split along its length) centrally located inside a standard rectangular-waveguide section excited in its fundamental TE_{01} mode. Both the ferrite rod and the polyfoam dielectric support make use of linear tapers at both ends for impedance matching. A thin resistive film, placed between the sections of the split rod and in a plane perpendicular to the input RF electric field, is used to attenuate the perpendicular component of this field generated in the magnetized ferrite rod. A low-current solenoid, wound around the rectangular-waveguide section, is used to supply the longitudinal magnetic control field.

An early model[5] of the modulator made use of a rectangular ferrite rod (0.280×0.300 inch) and an attenuating element consisting of a thin layer of

[3] R. C. LeCraw and E. G. Spencer, "Intrinsic Tensor Permeabilities of Ferrites Below Magnetic Saturation," DOFL TR-345; May, 1956.

[4] Ferramic R-1 ferrite, manufactured by General Ceramic Corp., has a dielectric constant (ϵ') of 13.6 and saturation magnetization ($4\pi M_s$) of approximately 2000 gauss.

[5] J. E. Tompkins, F. Reggia, and L. Joseph, "Multimode Propagation in Gyromagnetic Rods and its Application to Traveling Wave Devices," DOFL TR-861; Sept. 21, 1960.

aquadag (or carbon) on a 0.0002-inch thick mylar sheet. The low-current solenoid supplying the longitudinal control field was wound around the $\frac{1}{2}\times 1$-inch rectangular-waveguide section. The total length of the absorption modulator was 4 inches.

The isolation characteristics and input VSWR of the above model at 9250 Mc vs applied magnetic field are shown in Fig. 3. The width and length of the attenuating element were the same as those of the ferrite rod. Nearly constant electrical characteristics were obtained with this model over the frequency range of 7500 Mc to 10,500 Mc with the ferrite rod dimensions given in the figure. These electrical characteristics are reciprocal—that is, they do not depend upon the direction of propagation or magnetic control field.

As seen in Fig. 3, when the ferrite switch is operating in the OFF state, an isolation greater than 40 db is obtained, and this isolation is nearly independent of the magnitude of the magnetic control field. This characteristic is especially desirable in high-speed microwave switches. It is also interesting to note the similarity between this curve and the variation of the permeability component K' with applied field shown in Fig. 1. Thus, the simplified analysis leading to (4) gives a qualitative insight into the behavior of the ferrite rod in the absorption modulator.

The zero-field insertion loss is 0.5 db and the input VSWR remains less than 1.20 for all values of applied field over the operating frequency range. The total length of the modulator and the MgMn ferrite rod (including the impedance matching tapers) is 4 inches, and the dc power required to operate the modulator as a switch is approximately 2 watts.

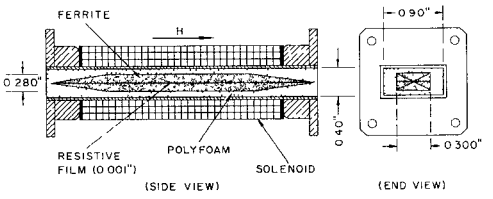

Fig. 2—Cross-sectional views of the ferrite absorption modulator.

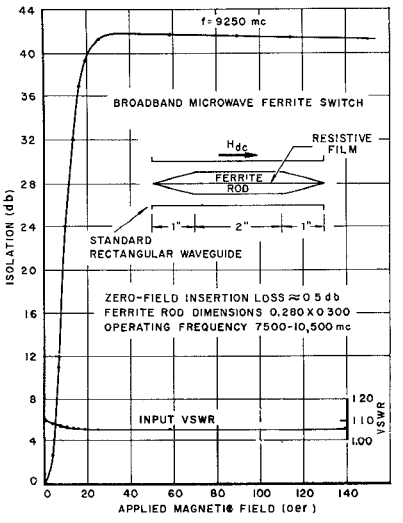

Fig. 3—Typical electrical characteristics vs applied longitudinal magnetic field. An aquadag resistive film on mylar was used as the attenuator element.

Improved Isolation-Bandwidth Characteristics

Because the resistivity of the aquadag film on the mylar sheet was not known and because its reproducibility and temperature characteristics were not good, a new type of attenuating element was devised which consisted of a specially selected mica sheet (0.001-inch thick) upon which was deposited a very thin film of pure metal. The resistivity of these attenuating elements was accurately known and could be adjusted over a wide range. Their temperature and frequency characteristics were also very good.

The first of these new attenuator elements which were used had a resistivity of 65 ohms per square. Beginning with these elements, an attempt was first made to optimize the isolation-bandwidth characteristics of the absorption modulator by adjusting the height and width of the ferrite rod. These results are shown in Figs. 4 and 5 for a number of MgMn ferrite rods in standard X-band rectangular waveguide (0.400×0.900-inch inside dimensions). The length of the ferrite rods and rectangular-waveguide sections was 4 inches.

Beginning with the ferrite rod dimensions given in Figs. 2 and 3 and making use of a metallized-mica attenuating element with a resistivity of 65 ohms per square, the maximum isolation of the absorption-modulator switch in the OFF state was measured from 7000 Mc to 11,000 Mc for a number of ferrite-rod heights and widths. The applied magnetic field used for these measurements was approximately 100 oersteds.

The measured data shown in Fig. 4(a) were obtained for three 0.300-inch wide ferrite rods with heights ranging from 0.280 inch to 0.300 inch. Only a slight improvement in the isolation characteristics is seen to occur at the low-frequency end. However, each of these rods was capable of giving an isolation of greater than 60 db over at least a 2000-Mc bandwidth. By optimizing the geometry of the attenuator element, isolations in excess of 70 db over a relatively narrow bandwidth (centered around 9500 Mc) were obtained with a rectangular ferrite rod having a height and width of 0.290 inch and 0.300 inch, respectively. The zero-field insertion loss of the above rods was approximately 0.5 db over the frequency range shown.

Further improvements in the isolation-bandwidth characteristics of the absorption modulator are shown in Fig. 4(b). Here we see the results for three ferrite rods, 0.320 inch wide, with heights also varying from 0.280-inch to 0.300 inch. A marked improvement in the isolation characteristics with height at the low-frequency end and a slight deterioration at the high-frequency end of the bandwidth are observed. The

increased isolation at the low-frequency end is due to an increase in the microwave energy concentration in the larger ferrite rods, while the dropping off of the isolation characteristics at the high-frequency end is due to higher-order modes propagating out of the attenuating region. Undulations in the isolation characteristics were also observed at the lower field values when operating at frequencies above 10,500 Mc.

Similar results obtained over the same frequency range are shown in Fig. 5 for several ferrite rods, each having a height of 0.300 inch. This time the width was taken as the parameter, increasing from 0.300-inch to 0.340-inch. No improvement was observed in the isolation characteristics by increasing the rod width above 0.320 inch. Thus, a ferrite rod 0.300 inch high and 0.320 inch wide was considered optimum over this frequency range. For this particular ferrite rod, the isolation in the OFF state was greater than 60 db over a bandwidth in excess of 2500 Mc and more than 55 db isolation was obtained over a 3500-Mc bandwidth. These characteristics can be extended to a higher frequency range by making use of techniques similar to

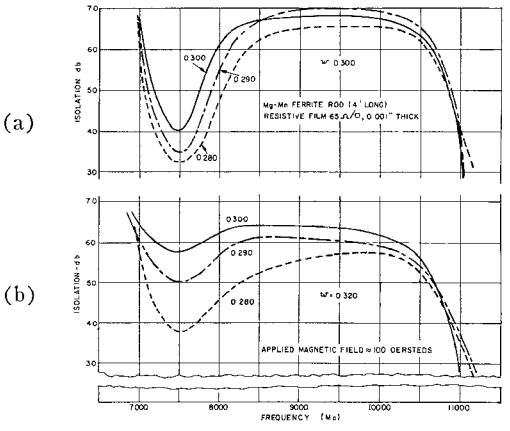

Fig. 4—Isolation-bandwidth characteristics of absorption modulator. Parameter was the ferrite rod height. (a) Rod width is 0.300 inch. (b) Rod width is 0.320 inch.

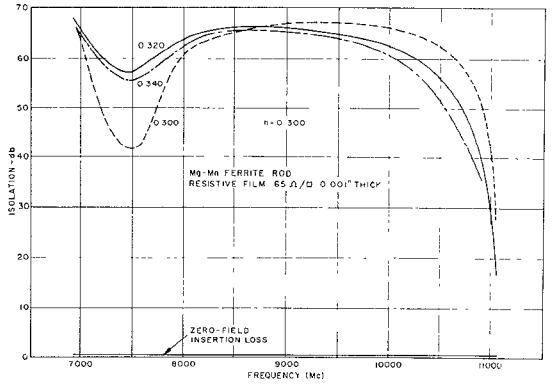

Fig. 5—Isolation-bandwidth characteristics using ferrite rods 0.300-inch high. The applied field was 100 oersteds and the rod widths varied from 0.300 to 0.340-inch.

that used with the rectangular-waveguide phase modulator,[1] *i.e.*, making use of a rectangular waveguide and ferrite rod with smaller cross-sectional dimensions. The zero-field insertion loss (approximately 0.5 db) is shown for comparison at the bottom of the figure.

The length and width of the attenuating elements which were used for the above measurements were the same as those of the particular ferrite rod used in the absorption modulator. It was found that attenuating elements which were wider and narrower than the ferrite rod resulted in higher zero-field insertion losses and narrower operating bandwidths, respectively. However, attenuator elements having a width slightly less than that of the ferrite rod are capable of isolations greater than that shown here.

The isolation characteristics from 8500 Mc to 9500 Mc of the rectangular-waveguide absorption modulator versus the applied magnetic field are shown in Fig. 6. These results were obtained with a 4-inch long rectangular ferrite rod, including 7/8-inch tapers at both ends, having a height and width of 0.300 inch and 0.320 inch, respectively. A metallized-mica attenuating element (0.001-inch thick) having a resistivity of 65 ohms per square was used between the split sections of the ferrite rod. As seen in the figure, the isolation characteristics did not vary greatly over this bandwidth, reaching a maximum value in excess of 60 db. Similar results, not shown, were obtained at 8000 Mc and 10,000 Mc. The input VSWR of this modulator at 9000 Mc, shown at the bottom of the figure, remained below 1.15 for all values of applied field. The solenoid current required to obtain the necessary magnetic-field strength is shown at the top of the figure. Approximately 2 watts of dc power were required to obtain a field strength of 40 oersteds.

Although (4) shows the permeability component K' to vary inversely with frequency, it is also true that the amount of energy concentrated in the ferrite rod ($\epsilon' = 13.6$) increases with frequency—one tending to cancel the effect of the other. Other factors contributing to the broad-band characteristics of the absorption modulator include the length and cross section of the ferrite rod, the thickness and width of the attenuating element, and, to a lesser degree, the resistivity of the attenuating element.

The ferrite modulator of Fig. 6 was subjected, in the OFF state, to an input CW power of 5 watts for a period of 3 hours. Very little change was observed in its isolation characteristics at this power level. In this state, essentially all the microwave power was dissipated in the metallized-mica attenuating element. Some deterioration of the polyfoam dielectric was observed at this power level, but this was corrected by using a low-loss silicone-foam dielectric. The peak power-handling capability of this ferrite modulator is approximately 5 kilowatts.

Data, shown in Fig. 7, were also taken at 9300 Mc to determine the isolation characteristics vs applied magnetic field of the absorption modulator for a number of ferrite-rod lengths and attenuator-element resistivities. These results were also used to determine the minimum length of the ferrite modulator necessary to obtain approximately 60 db isolation in the OFF state.

The curves in Fig. 7(a) show the isolation characteristics of the absorption modulator for several MgMn rods with lengths varying from $2\frac{1}{2}$ inches to 4 inches, including the impedance matching tapers at both ends. These rods had a cross-sectional dimension of 0.300 inch by 0.320 inch, and the resistivity of the attenuator element used for these measurements was 60 ohms per square. As seen in the figure, the maximum isolation obtainable increases rapidly with rod length up to 4 inches, and the effect of the demagnetizing field decreases with increasing rod length.

The curves in Fig. 7(b) were taken with a single ferrite rod, with dimensions given at the bottom, as the resistivity of the attenuator element was increased from 10 ohms to 80 ohms per square. Here we see that the maximum isolation which can be obtained increases rapidly until the resistivity reaches approximately 50 ohms per square, and decreases again as the resistivity is increased above this value. It is thus important to select the correct value of resistivity if good isolation characteristics are to be obtained. The value of resistivity chosen for a particular operating frequency also determines the phase-shift characteristics of the ferrite modulator.

Small discrepancies in the results shown here with those in preceding figures are probably due to differences in the taper lengths of the rods used, attenuating elements, and possibly even due to some variations in the ferrite material itself.

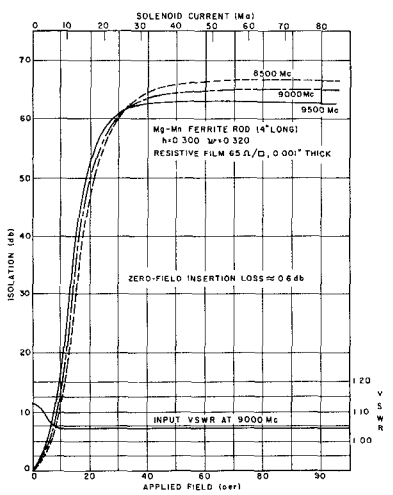

Fig. 6—Isolation characteristics of improved absorption modulator vs applied magnetic field.

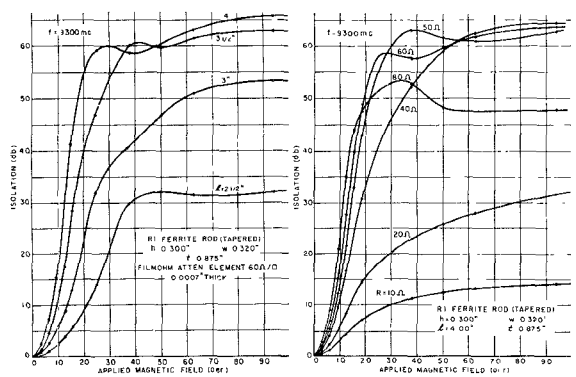

(a) (b)

Fig. 7—Isolation characteristics vs applied field for various ferrite-rod lengths and resistivities of attenuating element. (a) Parameter is rod length. (b) Parameter is attenuator-element resistivity (ohms per square).

Phase-Shift Characteristics

A final refinement of the absorption modulator is to adjust the resistivity of the attenuator element used with an optimum rod such that nearly zero phase shift occurs at the desired operating frequency. This has been accomplished at a number of frequencies between 8000 Mc and 9500 Mc.

The phase-shift characteristics of the absorption modulator at 9200 Mc for various values of resistivity of the attenuator element with a rectangular ferrite rod ($h = 0.300$ inch, $w = 0.320$ inch) are shown in Fig. 8. The metallized-mica attenuating elements between the split sections of the ferrite rod were 0.0006-inch thick, and their widths were the same as that of the rod. The magnitude of the applied magnetic field, not shown, increases from left to right along each of the phase-shift curves.

As seen in the figure, attenuator elements with very large values of resistivity give large phase shifts (lag) with applied magnetic field, similar to that which is obtained with the rectangular-waveguide phase modulator.[1] As the resistivity of the attenuator element is decreased, the phase shift obtained becomes small, ap-

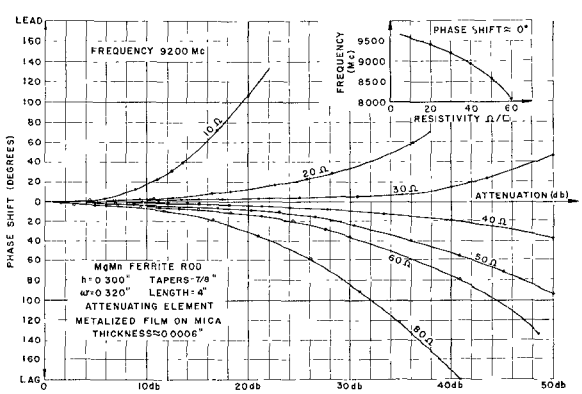

Fig. 8—Phase-shift characteristics of modulator using a 4-inch long ferrite rod (0.300×0.320 inch). Parameter is resistivity of attenuator element.

proaching zero for a resistivity of approximately 35 ohms per square. As the resistivity of the attenuator element is decreased below this value, the phase shift again begins to increase, but now a phase lead is obtained. As the resistivity is decreased to 10 ohms per square or less, the phase shift increases rapidly again, but the maximum insertion loss (or isolation) deteriorates very rapidly. This decrease in maximum isolation for large and small values of resistivity was also shown in Fig. 7.

The small insert at the top right of Fig. 8 shows the approximate resistivity of the attenuator element needed for a particular ferrite rod if nearly zero phase shift is to be obtained in the frequency range from 8000 to 9500 Mc. The most important region is from 20 ohms to 60 ohms per square. Thus, amplitude modulation with negligible phase modulation is possible with the above ferrite modulator. The length and width of the attenuator elements which were used for these measurements were the same as those of the ferrite rod, and their thickness was less than 0.001 inch.

Isolation Characteristics vs Temperature

The isolation characteristics of the rectangular-waveguide absorption modulator at 9350 Mc as a function of applied magnetic field are shown in Fig. 9 for a number of equilibrium temperatures from 33°C to 200°C. This modulator made use of a tapered ferrite rod (4 inches long), whose width and height were 0.320 and 0.300 inch, respectively. A silicone dielectric was used to support the rod at these high temperatures, and a 50-ohm per square resistive-attenuator element (0.001 inch thick) was used to dissipate the microwave energy in the OFF state. The dimensions of the attenuator element (approximately the same as that of the ferrite rod) were optimized for the 9000- to 10,000-Mc frequency range.

As seen in the figure, the isolation characteristics showed little deterioration with applied magnetic field for temperatures up to 100°C, reaching a maximum isolation in excess of 70 db. At 150°C, isolations greater than 60 db were still possible, but higher values of applied magnetic field were required. Above this temperature, however, the isolation characteristics deteriorate rapidly until the Curie temperature (290°C) is reached, at which time the ferrite medium becomes paramagnetic. These results are consistent with the known deterioration of the saturation magnetization of the ferrite material with temperature. The zero-field insertion loss of the absorption modulator remained nearly constant at 0.4 db for all temperatures up to 200°C.

Standard techniques were used to make the temperature measurements. An aluminum-constantan thermocouple was attached to the brass housing of the absorption modulator, which was placed in a 2-foot long electric oven. The EMF generated by the thermocouple was then measured as a function of temperature with a precision potentiometer. The modulator remained at each of the equilibrium temperatures shown in the figure for one hour before its isolation characteristics were determined.

A photograph of an early model of the absorption modulator described above is shown in Fig. 10. The two sections of the split ferrite rod and their dielectric supports are clearly seen in the foreground. The thin attenuator element, having the same length and width as that of the ferrite rod, is lying on top of the ferrite section nearest the modulator housing. Both ends of the ferrite rod and polyfoam dielectric supports are tapered for impedance matching.

As seen in the photograph, the ferrite modulator has axial symmetry which is necessary for reciprocal microwave characteristics. The low-current solenoid supplying the longitudinal magnetic control field is wound around the $\frac{1}{2}\times 1$-inch rectangular-waveguide section and is potted in an Epon resin. The total length of the modulator is 4 inches.

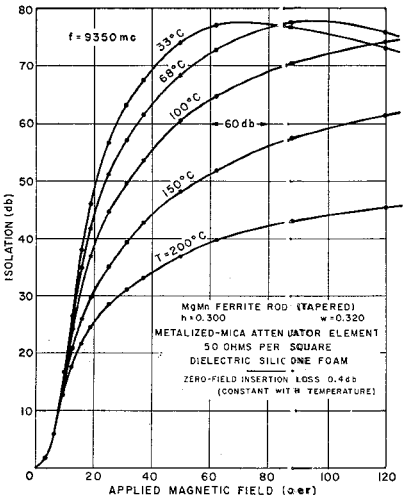

Fig. 9—Isolation characteristics of the absorption modulator vs ambient temperature from 33°C to 200°C.

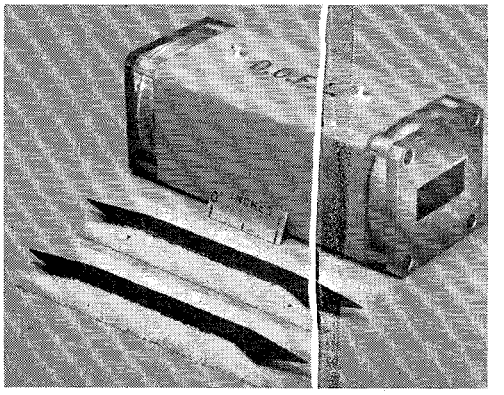

Fig. 10—Photograph of broad-band absorption modulator. Total length of modulator is 4 inches.

Conclusion

A new ferrite absorption modulator has been developed for high-speed switching of microwave power. This high-speed amplitude modulator makes use of a longitudinally magnetized ferrite rod (split along its length) centrally located inside a standard rectangular waveguide excited in its fundamental TE_{01} mode. A thin resistive film, placed between the sections of the split ferrite rod and perpendicular to the input RF electric field, is used to attenuate the perpendicular mode generated in the magnetized ferrite rod.

Several fiber-glass waveguide models of this absorption modulator, with a 0.0005-inch thick silver plating on the inside, have been designed for sine-wave modulation frequencies up to 100 kc. These units make use of a modulating solenoid (with ferrite-rod loading) which is self-resonant at the desired modulating frequency. Because of the small electrical inertia associated with its low-field solenoid, these ferrite modulators can be designed for switching microwave energy in less than 1 μsec with noncritical magnetic control fields.

Other important applications of the absorption modulator described above include an electrically controlled variable attenuator for automatically stabilizing the amplitude of FM oscillators, pulse shaping of the microwave energy and high-speed TR switching in microwave radar systems.

Rectangular Waveguide Theoretical CW Average Power Rating*

H. E. KING†, SENIOR MEMBER, IRE

Summary—**A theoretical CW average power rating, limitation imposed by a temperature rise resulting from power dissipation within the rectangular waveguide walls, can be determined by predicting the rise in temperature. Formulas for the evaluation of the CW average power rating have been developed and are presented here, and the power rating curves are given for the WR-2300 waveguide (320 Mc) through the WR-19 waveguide (60 kMc).**

Localized hot spots, associated with a standing wave on a mismatched waveguide, require a derating factor. The axial flow of heat from these high current spots has been considered in calculating and plotting this derating factor.

I. Introduction

THE major power rating consideration in present waveguide designs, using the TE_{10} mode, has been the limitation imposed by voltage breakdown (peak power rating). However, with the advent of high average power microwave systems, the average power rating of waveguides should be considered for future designs. The average power rating is determined by imposing a specified temperature rise in the conducting wall of the waveguide. High average RF power can be obtained by systems using high power generators or an array of generators united through a power combiner.

This paper presents formulas and curves that can be used to determine the average power rating of rectangular waveguides.[1] The rating is defined by choosing an arbitrary limit for the temperature rise with the waveguide in an environment of still air. (The average power rating can be raised, if desired, by choosing a higher temperature limit and using forced cooling.)

High current points, associated with a voltage-standing wave, on a mismatched waveguide cause additional increases in temperature. Therefore, a derating factor as a function of the standing wave ratio (VSWR) has been plotted. This derating factor takes into account the axial flow of heat from the high current point.

II. Theory

A. Power Rating of a Waveguide

The approach to determining the average power rating is to find the attenuation per unit length. With the attenuation known, the dissipated power in the walls of the matched waveguide may be found where a given power is being transmitted through it. The dissipated

* Received by the PGMTT, December 13, 1961; revised manuscript received, May 4, 1961. A portion of the work reported in this article was performed under U. S. Air Force Contract AF 04(647)-619.

† Aerospace Corp., Los Angeles, Calif.; formerly with Space Technology Labs., Inc., Los Angeles.

[1] The average power rating of coaxial cable has been treated by W. W. Macalpine, "Heating of radio frequency cables," *Elec. Commun.*, vol. 25, pp. 84–89; March, 1948.